ELSEVIER

Contents lists available at ScienceDirect

# **Optics Communications**

journal homepage: www.elsevier.com/locate/optcom



# Photonic implementation of a highly reconfigurable wideband RF spectral shaper



Jia Ge, Daniel A. Garon, Mable P. Fok\*

Lightwave and Microwave Photonics Laboratory, College of Engineering, University of Georgia, Athens, GA, 30602, USA

#### ARTICLE INFO

#### Keywords: Microwave photonics RF spectral shaper RF spectrum shaping Reconfigurable RF filter RF spectral equalization

#### ABSTRACT

In emerging Radio Frequency (RF) systems, the capability to dynamically process a wide range of frequency bands is highly desired due to the multi-frequency operation in multi-function RF systems and the large signal bandwidth usage associated with data-intensive applications. As the operation bandwidth increases, the frequency response uniformity of both RF components and microwave transmission medium degrades, that leads to the need of broadband RF spectrum equalization to support wideband high-quality services. Therefore, a wideband and reconfigurable RF spectral shaper is highly desired for dynamically manipulating the RF spectrum from low- to high-frequency band. Unfortunately, it is very challenging for conventional RF electronics to achieve dynamic spectral control over a wide operation bandwidth. In this paper, we take advantages of photonics and demonstrate a highly-reconfigurable RF spectral shaper that can manipulate an RF spectrum of tens of GHz wide. The proposed scheme is based on a microwave photonic filter architecture with multiple tunable, reconfigurable and switchable passbands. By manipulating the shape, bandwidth, and frequency of the passbands, highly reconfigurable wideband frequency responses for spectral equalization are experimentally achieved, covering the entire 0 to 10 GHz frequency range with adjustable attenuation up to 40 dB. Various RF equalization functions including tunable positive/negative slope, non/inverted parabolic, and multi-point spectral control with tunable floor are experimentally demonstrated using the proposed system. Several of the demonstrated RF functions have also been applied to arbitrary pulse shaping. The RF spectral shaper can be tuned to adapt to different scenarios dynamically, which could benefit a variety of applications including RF signal processing systems and communication networks.

#### 1. Introduction

Radio frequency (RF) wideband signal processing is essential for a variety of fields including emerging communication systems, wideband radar, and multiband satellite systems [1,2], where the capability to freely process a wide range of frequency components is highly desired. One example is to equalize and balance the non-uniform frequency response of wideband RF components and transmission medium. Due to the inherent limitations of RF electronics, the gain or loss of RF components varies a lot at different frequency bands, which is a very common and thorny issue. The most commonly used components - RF cables and amplifiers - have uneven loss/gain curves over frequencies that vary between different manufacturers [3-5]. Therefore, it is extremely difficult to optimize the wideband performance of a RF system that consists of various RF components, resulting in a limited operation bandwidth and degraded performance. Similar situation happens in multiband communication networks, where multiple channels that are spread across a wide frequency range are transmitted at the same time [6,7]. Furthermore, carrier frequencies could have to change over

time to meet the channel requirement, the uneven losses during transmission at different frequency would result in tremendous differences in the received power, and thus greatly deteriorate the received signal quality. In these cases, a wideband and reconfigurable RF spectral shaper is required to compensate and balance the frequency dependent gain/loss to improve system performance. Another scenario commonly found in communication and RF systems is the need of reshaping an existing RF signal or spectrum into a different profile for transmission or processing purpose, applications include spectral shaping for dynamic spectrum access in wireless network [8], channel crosstalk reduction in communication systems [9], as well as arbitrary waveform shaping in radar system and biological imaging/spectroscopy [10]. To dynamically shape the waveform and spectrum, a reconfigurable RF spectral shaper that can tailor and shape the RF components is required.

Unfortunately, it has not been successful to implement an RF spectral shaper or equalizer using RF electronics. Currently, conventional electronics-based approaches use a combination of tunable attenuators,

<sup>\*</sup> Corresponding author.

E-mail address: mfok@uga.edu (M.P. Fok).

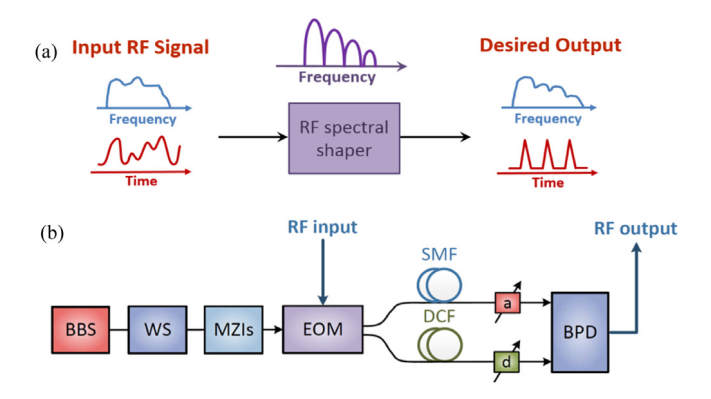


Fig. 1. (a) Illustration of the proposed RF spectral shaping based on a MWP multiband filter. (b) Schematic diagram of the photonics based reconfigurable RF spectral shaper. BBS: broadband source; WS: waveshaper; MZI: Tunable Mach–Zehnder interferometer; EOM: electro-optic modulator; SMF: single-mode fiber; DCF: dispersion compensating fiber; BPD: balanced photo-detector.

RF switches and bandpass/bandstop filters [5,11] to achieve simple shaping functions. Therefore, most of the resultant spectral shaping functions are either fixed or with limited amplitude and compensating slope tunability over a narrow bandwidth through the adjustment of attenuation coefficient. Furthermore, physically switching between different configurations is needed to reconfigure the spectral shaping functions. Existing spectral shaping approaches can only achieve simple shaping functions, such as linear slope and first-order parabolic shaping for compensating small frequency dependency in RF cables. A more comprehensive spectral shaper with reconfigurable spectral functions and multiple spectral control points are desired for versatile applications. The key for achieving a RF spectral shaper with high reconfigurability and comprehensive functionality requires dynamic control of the frequency, slope (i.e. bandwidth), and amplitude of the multiple spectral control points over a wide frequency range, which can be ideally achieved by a highly tunable/reconfigurable RF filter with multiple passbands. Unfortunately, such kind of RF filter is extremely difficult to achieve with current technology due to the lack of tunability in RF electronics and the challenges to simultaneously satisfy the design parameters for multiple passbands over a wide frequency range [12]. State-of-the-art electronic approaches can achieve multiband filters with a maximum of six fixed passbands [13,14] as well as tunable tri-/quad-band filters with limited frequency tuning range and passband reconfigurability [15-17]. A promising way to implement an RF multiband filter with flexible passband reconfigurability and wide frequency tuning range is critical for achieving the desired dynamic and comprehensive RF spectral functions.

Turning to photonics for solutions, microwave photonics (MWP) technique has been considered as a promising candidate to many challenging tasks in RF electronics [1,2,18-21], due to its unique properties including wide operation bandwidth, flexibility, and tunability. Photonics provides the flexibility requirement urgently needed in current and future RF systems, which is proven by the recent attentions on reconfigurable photonic systems [22,23]. For example, microwave photonic approaches for generating arbitrary RF waveform generation have been successfully demonstrated [24-26], through line-by-line optical spectral shaping of an optical frequency comb using spatial light modulator [27,28], or based on frequency-to-time mapping in a dispersive medium [29]. Instead of focusing on the generation of newly arbitrary shaped pulse, direct manipulation of existing RF spectral composition is highly desired due to its ability to customize the transmission channel, and its high demand in nearly all RF systems. Recently, a programmable microwave spectral shaper has been demonstrated based on bandwidth scaling technique [30] which the RF spectrum was stretched in optical domain to achieve fine spectral resolution in megahertz range.

The scheme uses a coherent optical frequency comb and a Vernier comb filter for bandwidth scaling and achieves single-point shaping functions of bandpass filter, notch filters, and triangle bandpass filter over a bandwidth of 1.5 GHz with out-of-band rejection of 20 dB. Reconfigurable and programmable microwave photonic filters with adjustable passband profiles have also been demonstrated [30-42], which could be a promising candidate for RF spectral shaping. However, most of the reconfigurable microwave photonic filters are limited to single bandpass operation with limited frequency range. Microwave photonic filters with multiple reconfigurable passbands are not trivial to achieved and not every MWP filter approach could be scalable to a multiple passband scheme [43]. Multiple tunable and reconfigurable passbands are essential to provide multiple spectral control points for wideband RF spectral shaping and equalization purpose. Examples of existing MWP multiband approaches include tunable/reconfigurable multiband MWP filters with two or three passbands [43-47], a MWP multiband filter with independently reconfigurable passband spectral properties [48], and a MWP multiband filter that we demonstrated with 12 switchable passbands at fixed frequencies [41]. Although microwave photonic signal processing technique has shown its enormous potential over conventional RF electronic counterpart, RF spectral shaping and equalization based on microwave photonics has not been fully explored.

In this article, a comprehensive photonics-based RF spectral shaper with highly reconfigurable functionalities is proposed and demonstrated. A photonic based RF spectral shaper with 4 independent spectral control points, customizable and continuous frequency control across a 10 GHz bandwidth, as well as -40 dB dynamic and continuous amplitude control is designed to achieve wideband and reconfigurable spectral shaping curves. Compared with existing microwave photonic spectral filtering [31-41,43-49] and spectral shaping [30,42,50] approaches, the scheme presented here mainly focuses on the use of microwave photonic multiband filter technique for reconfigurable RF spectral shaping and equalization purposes, as well as explores a comprehensive list of potential spectral functions. Various spectral shaping functions are demonstrated, including positive/negative linear slopes with variable slope steepness, tunable parabolic and inverted parabolic responses, bandpass filter with variable filter profiles, as well as complex and multiple-peak spectral shaping. The demonstrated RF spectral shaper shows high operation flexibility that the shaping functions can be reconfigured, tuned, and switched without any replacement of hardware.

## 2. Architecture and operation principle

RF spectral shaping can be achieved by precisely tailoring the frequency components of a RF signal using a desired spectral profile, thus, the waveform in time can also be shaped correspondingly. As shown in Fig. 1(a), the key and challenge for RF spectral shaping is to generate reconfigurable RF responses with the desired frequency profiles. Here, the proposed RF spectral shaper is based on a tunable MWP multiband filter with full control of its frequency, amplitude, spectral profile, and number of spectral control points (i.e., multiple filter passbands). The schematic diagram of the experimental setup is shown in Fig. 1(b). A superluminescent diode with 22 mW output power and 40 nm spectral width is used as the broadband light source (BBS), which is spectrally shaped by a waveshaper and sliced by cascaded Mach-Zehnder interferometers (MZI). The envelope profile of the multi-wavelength optical comb is shaped by the waveshaper, that in turn controls the RF spectral profile of each RF spectral control point. The spectrally sliced BBS acts as the multiwavelength optical carrier. Each MZI consists of a continuously tunable coupler and a tunable delay line, such that the number of interleaving optical comb as well as the amplitude and wavelength spacing of the multi-wavelength optical comb can be adjusted continuously. Unlike other approaches that use a waveshaper as the spectral slicer [48] which has limited resolution that constrains design flexibility and out-of-band suppression ratio, our scheme provides continuous amplitude and frequency tuning due to the continuous tunability of the cascaded MZIs. Each stage of the tunable MZI has an insertion loss of ~6.5 dB. The MZIs determine the number of spectral control points, control point frequency, and control point amplitude. RF input signal is modulated onto this shaped multi-wavelength optical carrier through a 12 Gb/s dual-drive Mach–Zehnder electro-optic modulator (EOM), then the modulated optical carrier is split into two branches. A phase modulator can be used instead if the baseband response is not desired. The upper branch consists of a dispersive medium which provides linear time delays across all the taps in the modulated optical carrier, as a result, RF bandpass filter response is formed at the photo-detector due to finite impulse response (FIR).

In this experiment, a 4.1-km dispersion compensating fiber (DCF) with a dispersion coefficient of -149.36 ps/(nm.km) at 1530 nm is used for providing dispersion. The bottom branch consists of a piece of single-mode fiber (SMF) which is used to match the lengths between the two branches. Since the SMF has negligible dispersion compared to the DCF, all-pass RF response is resulted from the bottom branch alone after photo-detection. In our experiment, a 20-GHz balanced photodetector (BPD) with responsibility of 0.8 A/W is used to combine the all-pass response and bandpass response. To increase the degree of freedom of the spectral shaper, a tunable optical attenuator is used for precisely adjusting the amplitude ratio between the two branches as well as disabling the all-pass response branch if needed, while an optical delay line is used to precisely adjust the phase between the two branches for achieving addition or subtraction between them at the balanced photo-detector. Frequency response of the proposed RF spectral shaper is measured by a 20-GHz network analyzer with an intermediate frequency bandwidth of 5 kHz. The proposed spectral shaper setup enables multi-spectral-point control with adjustable control point frequency, spectral width, and amplitude. The tunability of the spectral control points determines the reconfigurability of the RF spectral shaper, which is extremely challenging with electronics. Our multiple-adjustable control point design is desired to flexibly balance or manipulate the amplitudes of the spectrum at different frequency bands, which can hardly be achieved with electronics.

Frequency response of a FIR filter can be expressed as the summation of a series of weighted and delayed replica of the original RF signal (i.e. taps of the FIR) [34]:

$$H(\Omega) \propto \sum_{n=1}^{N} a_n e^{-j\Omega nT}$$
 (1)

where  $\Omega$  is the RF frequency, N is the number of taps of the FIR filter,  $a_n$  is the amplitude (weight) of the nth tap of the optical comb, and T is the differential delay between each adjacent tap:

$$T = \Delta\omega \cdot \beta_2 \cdot L_D \tag{2}$$

In a microwave photonic based FIR filter, the taps are formed by each spectral line in the optical comb, and the delay T is determined by the frequency spacing ( $\Delta\omega$ ) of the optical comb and the total dispersion of the dispersive medium — governed by the group velocity dispersion ( $\beta_2$ ) and length of the DCF ( $L_D$ ) of the dispersive medium. The center frequency ( $\Omega_0$ ) of each spectral control point (i.e. passband frequency) is determined by the two cascaded tunable MZIs, which is governed by Eq. (3),

$$\Omega_0 = \frac{2\pi}{\beta_2 L_D \Delta \omega} \tag{3}$$

For a system where the total dispersion is fixed, center frequency of each spectral control point is solely determined by the frequency spacing of the optical comb, which can be controlled continuously by adjusting the delay line inside the MZI. To achieve multiple spectral control points, multiple spectrally interleaved optical combs with different comb spacings are needed to be generated at the same time [46]. With two cascaded MZIs, high-order optical comb that consists of four

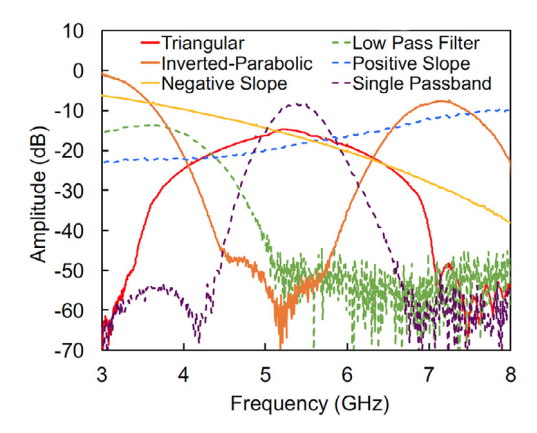


Fig. 2. Various RF spectrum shaping functions achieved by the proposed RF spectral shaper.

interleaving optical combs at different comb spacings can be generated, such that 4 tunable spectral control points are resulted. Spectral width  $(\delta \Omega_{3dB})$  of each control point is adjustable and is governed by Eq. (4) when the dispersion slope of the DCF is negligible,

$$\delta\Omega_{3dB} = \frac{\sqrt{8\ln 2}}{\beta_2 L_D \Delta\omega} \tag{4}$$

where  $\delta\omega$  represents the overall bandwidth of the optical comb. As shown, the 3-dB spectral width of the control point is inversely proportional to the overall bandwidth of the optical comb, which is adjustable through controlling the optical comb bandwidth by the waveshaper. Last but not the least, the frequency response of each spectral control point can be derived from Eq. (1), which is governed by the weight and delay of the taps. Thus, the spectral profile ( $S(\Omega)$ ) of each spectral control point can be precisely tailored by controlling the overall envelop of the optical comb ( $S(\omega)$ ) through a Fourier transform relationship [30,42,48,50] using the waveshaper, as shown in Eq. (5).

$$S(\Omega) \propto \int_{-\infty}^{\infty} S(\omega) \cdot e^{j\beta_2 L\Omega\omega} d\omega = \mathcal{F}[S(\omega)]$$
 (5)

Noticing that the spectral resolution of the waveshaper is only 10 GHz, which is not fine enough to directly shape the RF spectrum in optical domain — meaning that line-by-line spectral shaping will not work through the use of a waveshaper. Therefore, the waveshaper is only used for controlling the overall profile (i.e. Gaussian, flat-top and chirped passband profile) of each control points by manipulating the envelope of the multi-wavelength optical carriers, while the multi-wavelength optical carrier generation is taken care by the cascaded MZIs. Utilizing both the tunable cascaded MZIs and the waveshaper enable the implementation of an RF spectral shaper with multiple highly reconfigurable and tunable control points.

#### 3. Results

In this article, we experimentally demonstrated various tunable RF spectral shaping functions including positive/negative linear compensations, parabolic and inverted parabolic equalizations, triangular and Gaussian filtering, low pass filtering, as well as complex and multiple-peak spectral shaping. Fig. 2 shows examples of the spectral shaping functions that can be achieved by our proposed RF spectral shaper. The detailed design, configurations and functionalities of the proposed RF spectral shaper for different functions are shown in Table 1 and will be described in detail as follow.

**Table 1**Demonstrated spectrum shaping functions based on different configurations of the proposed RF spectral shaper.

Function	All-pass branch	Bandpass branch	Number of control point	Reconfigurability
All-pass floor	Enabled	Disabled	0	Tunable attenuation
Positive linear response	Disabled	Enabled	1	Tunable slope
Negative linear response	Disabled	Enabled	1	Tunable slope
Parabolic response	Disabled	Enabled	1	Tunable frequency and bandwidth
Inverted-parabolic response	Disabled	Enabled	2	Tunable frequency and bandwidth
Bandpass response	Disabled	Enabled	1–4	Tunable frequency, bandwidth and passband count
Bandstop response	Enabled	Enabled	1–4	Tunable frequency, bandwidth and notch count
Low-pass response	Disabled	Enabled	1–4	Tunable bandwidth
Saw-tooth response	Disabled	Enabled	1–4	Tunable profile, bandwidth and peak count

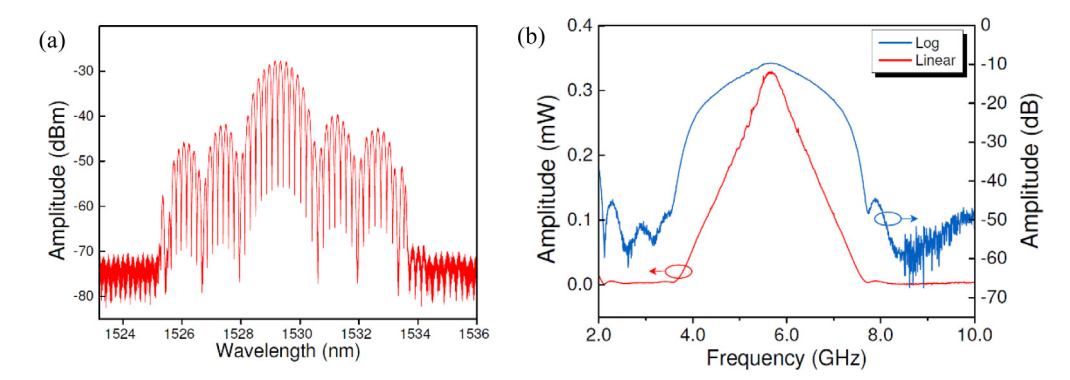


Fig. 3. Triangular passband generation. (a) Optical multi-carrier frequency comb with a Sinc-square profile. (b) Generated MWP bandpass filter with a triangular profile, plotted in both linear (red) and log (blue) scale. (For interpretation of the references to color in this figure legend, the reader is referred to the web version of this article.)

#### 3.1. Linear equalization

We first investigate the implementation of linear equalization curves with positive and negative tunable slopes, which are commonly used for compensating linear losses in systems where large scales of waveguides or RF cables are used. To achieve linear equalization curves with tunable slopes, the spectral shaper is configured to generate either a triangular or Gaussian RF spectral profile and is tuned to align the desired edge to the frequency range of interest, i.e. the rising edge forms a positive slope while the falling edge forms a negative slope. The choice of RF spectral profile depends on the exact shape of the RF response that is needed to be compensated. To generate a triangular RF spectral profile at the spectral shaper, envelope of the 8-nm multiwavelength optical carrier generated from a single stage MZI is shaped to a Sinc-square profile using the waveshaper, as shown in Fig. 3(a). Since the Fourier transform of a Sinc-square function is a triangular function, a triangular RF spectral profile is resulted at the spectral shaper, as shown in Fig. 3(b). The resultant spectral profile of the spectral shaper is plotted in both linear (red) and logarithmic (blue) scales, which shows a triangular profile with both positive and negative linear slope edges (in linear amplitude scale) been generated successfully. In our demonstration, the 2nd MZI stage is disabled by setting the input optical coupler to 100:0 ratio, while the all-pass branch before the balanced PD is switched off (i.e. applying a large attenuation at the attenuator) to disable the addition/subtraction function.

To generate a negative slope equalization curve, a baseband filter with a Gaussian profile is generated such that the right portion of the passband is served as the negative equalization curve, as shown in Fig. 4(a). Slope of the negative equalization curve is tunable by controlling the bandwidth of the Gaussian passband through the tuning of the multi-wavelength optical carrier bandwidth ( $\delta\omega$ ). Fig. 4(a)

shows the experimental results of the negative equalization curves with different slopes ranged from -13.3 dB/GHz to -4.2 dB/GHz. Then, a triangular passband is used to generate a positive slope equalization curve, center frequency of the triangular passband is set to the highest frequency of the frequency range of interest, such that the left portion of the passband serves as the positive equalization curve. As shown in Fig. 4(b), slope of the positive equalization curve is tunable from 25.2 dB/GHz to 6.9 dB/GHz by controlling the bandwidth of the triangular/Gaussian passband. Both the positive and negative equalization curves are linear in linear amplitude scale and can be adjusted to cover different frequency ranges and up to 50-dB compensation depth is obtained.

#### 3.2. Parabolic shaped equalization

Half-sine parabolic shaping curves are primarily used to compensate the gain variations in wideband devices or systems where the maximum amplification/attenuation occurring at the mid-band, such as traveling-wave-tube amplifiers and solid-state amplifiers. Parabolic shaped compensation curves can be generated by the design of a Gaussian profile at the spectral shaper, i.e. the multi-wavelength carrier envelope is also a Gaussian shape. Again, the all-pass branch is switched off since a Gaussian profile can be generated directly from the bandpass branch. As shown in Fig. 5(a), different parabolic compensation curves covering various frequency ranges are achieved through the adjustment of the envelope bandwidth of the multi-wavelength optical carrier ( $\delta\omega$ ). Out-of-band suppression of over 50 dB is achieved. The equalization curves are centered at 5.0 GHz, and can be tuned to different center frequencies by adjusting the optical tunable delay line in the tunable MZI. Furthermore, inverted-half-sine parabolic can be achieved through

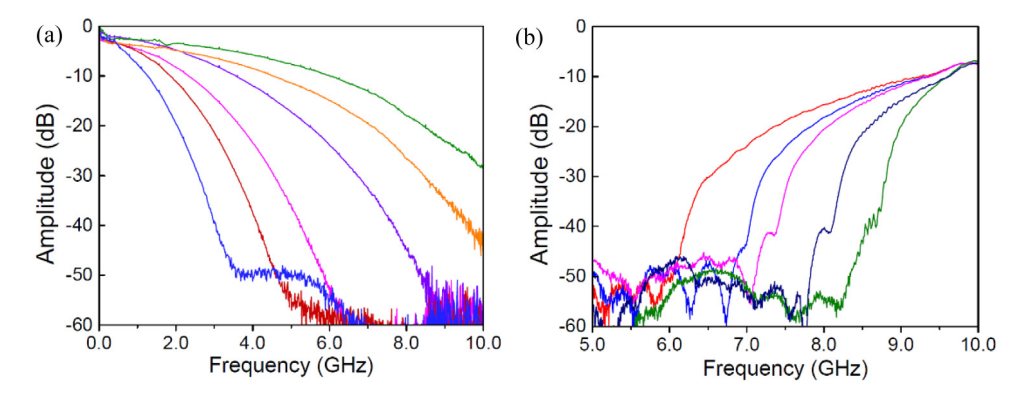


Fig. 4. Linear compensation curves with tunable slopes. (a) Negative slopes. (b) Positive slopes.

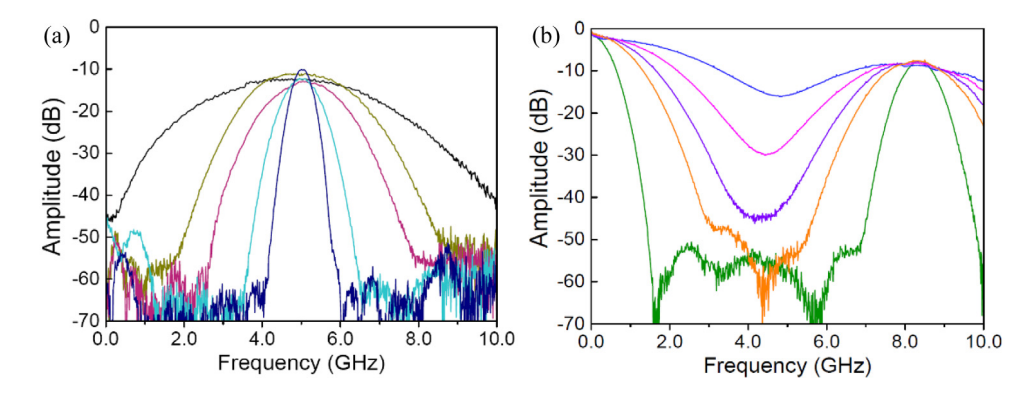


Fig. 5. Demonstration of parabolic and inverted-parabolic equalization functions. (a) Parabolic compensation curves with various compensation slopes. (b) Inverted-parabolic compensation curves with various compensation slopes and depths.

the combination of two Gaussian profiles at two spectral control points. By adjusting the center frequency and bandwidth of the two Gaussian spectral profiles, compensation curves with tunable depths and slopes can be obtained, as shown in Fig. 5(b). The compensation depth is adjustable from 10 dB to 50 dB when Gaussian profiles with different spectral bandwidths are used.

# 3.3. Tunable attenuation floor

The additional all-pass branch before photo-detection is to allow the spectral shaper to have a tunable spectral floor over the whole frequency range of interest. By switching off the bandpass response branch, frequency response of the all-pass branch is measured and is shown by the black solid curve in Fig. 6(a). A flat response over the whole 10 GHz range is observed with less than 1 dB of amplitude variation. This tunable spectral floor provides additional flexibility to adjust the compensating depth in any spectrum shaping functions that are generated from the spectral shaper. Furthermore, through the control of the relative phase between the bandpass branch and allpass branch using a tunable optical delay line, addition or subtraction operation between the two branches can be achieved. The rest of the solid curves in Fig. 6(a) show the frequency response of the spectral shaper when double-Gaussian spectra (one at 0 GHz and one at 7 GHz) are combined with different levels of spectral floor (i.e. addition operation). Amplitude of the spectral floor is adjustable by -60 dB through the control of optical tunable attenuator in the all-pass branch. Correspondingly, the subtraction between the two branches is shown by the pink dashed curve in Fig. 6(a), where a notch filtering response is achieved to cut out the undesired frequency band from the spectrum.

# 3.4. Arbitrary spectrum shaping with multiple control points

The shaping functions described above are achieved using just one MZI for the generation of multi-wavelength optical carrier, which composes the basic functions of the RF spectral shaper. However, wideband and multiband RF systems usually require more complex shaping functions with different compensation depths to satisfy the discrepancy between various frequency bands. In this case, multi-point RF spectral shaping is desired to manipulate the powers between different frequency bands. Based on various combinations of the basic spectral functions generated by the spectral shaper, complex spectral shaping functions can be achieved when multiple spectral control points are obtained using cascaded MZIs. Low-pass filter response with tunable bandwidth is first implemented by two spectral control points and both with Gaussian profile, i.e. one centered at 0 GHz and one centered at a higher frequency. Through the control of the bandwidth and center frequency of the two Gaussian spectral points, the 3-dB bandwidth of the low-pass filter is adjustable from 2.5 GHz to 7.0 GHz, as shown in Fig. 6(b). Next, four spectral control points and a baseband spectral point are generated based on two cascaded MZIs as shown in Fig. 7(a). In this example, center frequencies of the four spectral control points are set to locate evenly within the 10 GHz frequency range of interest. Meanwhile, both the frequency and amplitude of the spectral control points are tunable through various settings of the cascaded MZIs. The equalization functions shown in Fig. 7(a) are used in multiband communications, where five frequency bands (baseband, 2.2 GHz, 4.4 GHz, 6.6 GHz and 8.8 GHz) are transmitting at the same time. Through the control of the spectral profile, bandwidth, and center frequency of each spectral control points, as well as the power and phase of the all-pass branch, various complex spectral shaping functions can be achieved. Two examples are shown in Fig. 7(b) - the purple curve is a multiband notch filter to remove multiple undesired bands, while the red curve is a saw-tooth-like function for spectrum shaping in signal processing applications. It is worth noticing that there is a discrepancy in amplitude between each of the peak in high-order spectrum shaping functions. The lower power peaks are contributed from the optical comb generated from the second-order product of MZI1 and MZI2.

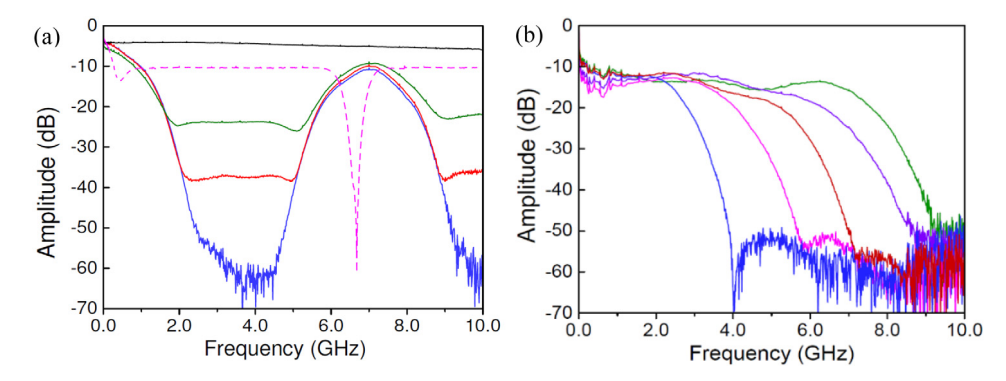


Fig. 6. (a) Bandpass response with tunable attenuation floors. (b) Low-pass response with tunable bandwidths. (For interpretation of the references to color in this figure legend, the reader is referred to the web version of this article.)

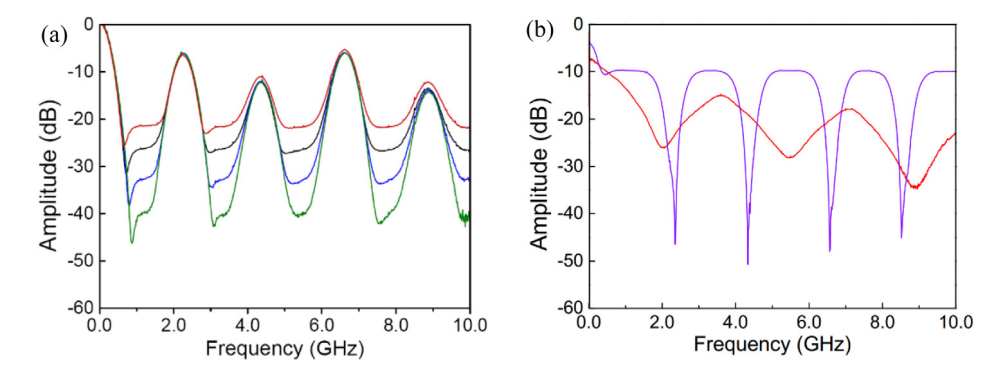


Fig. 7. High-order spectrum shaping functions with multiple control points. (a) Equalization function with four bandpass responses and different tunable noise floors. (b) Multi-notch response and saw-tooth-like response. (For interpretation of the references to color in this figure legend, the reader is referred to the web version of this article.)

Second-order product optical comb has weaker extinction ratios and results in lower amplitude in RF domain.

# 3.5. Arbitrary pulse shaping based on the reconfigurable RF spectral shaper

To demonstrate the capability and performance of manipulating a wide range of frequency component, the proposed RF spectral shaper is tested for arbitrary pulse shaping. A 125 Mbit/s square-like pulse train is used as the original pulse and is launched into the RF spectral shaper for reshaping, the corresponding RF spectrum and waveform before shaping are shown in Fig. 8(a). A low-pass spectral function with Gaussian profile is generated by the spectral shaper and is used to shape the RF spectrum of the square-like pulse train, such that the higher frequency components beyond 1 GHz are removed, as shown in Fig. 8(b). The square pulse is successfully shaped into a Gaussian profile, as shown by the inset in Fig. 8(b). When the spectral shaper is set to have a Sinc-square spectral shape, it reshapes the RF spectrum as shown in Fig. 8(c) and a triangular temporal profile is resulted. To generate the Sinc-square spectral profile, 4 spectral control points are used to adjust the frequency components, such that a triangular pulse train is generated in the time domain. Both the 3-dB bandwidth and the slope of the triangular pulse can be adjusted by precisely tailoring the corresponding frequency components through the RF spectral shaper. The insertion loss of the spectral shaper is about 4-10 dB across the 10 GHz frequency range, which is compensated by an erbium-doped fiber amplifier. As a result, the noise floors of the reshaped pulses are ~5 dB higher than the original pulse, as observed in Fig. 8(b) and 8(c).

#### 4. Discussion

Dynamic and wideband RF spectral shaping is essential in both current and emerging RF systems. Multiple spectral control points and high reconfigurability are the core of the proposed RF spectral

shaper, which are achieved through cascaded tunable MZIs. With the use of two serially cascaded tunable MZIs, 4 different spectral control points are obtained to cover a 10-GHz operation range. Increasing the number of cascaded MZIs will significantly increase the number of simultaneous spectral control points, which will in turn enhance the flexibility, resolution and operation range of the spectral shaper. For example, 3 serially cascaded MZIs will result in 13 different control points [51], and 49 control points can be obtained when 4 MZIs are used. Furthermore, 2-dimensional MZI mesh structure [22,23,52] can be implemented by cascading the tunable MZI in both parallel and serial configurations, such that the reconfigurability of the spectral shaper can be further enhanced - increasing the number of possible spectral control point combinations. MZI - the key and basic unit of the RF spectral shaper, has been successfully integrated into photonic chips through various techniques [52–56]. Therefore, it is promising to integrate the proposed RF spectral shaper into a chip scale with a larger number of cascaded MZIs in a 2-dimensional mesh structure, to achieve a programmable microwave photonic spectral shaper for wideband and multiband RF signal processing.

There are several aspects of the proposed RF spectral shaper that could be further improved. First, spectral resolution can be increased by cascading more MZIs in both serial and parallel configurations to increase the number of spectral control points over the target frequency range. Bandwidth scaling technique [30] could also be used in the proposed RF spectral shaper to increase spectral resolution through spectral stretching. Second, flexibility of the spectral shaper can be further increased by enabling independent manipulation of each spectral control point through the use of an optical spectral slicer and a new optical comb design algorithm [48]. It has been demonstrated that spectral properties of each passband, including spectral shape, frequency, bandwidth, amplitude, and group delay slope, in a multiband microwave photonic filter can be independently controlled. Lastly, system integration [31,52–56] could significantly improve SWaP of the RF spectral shaper.

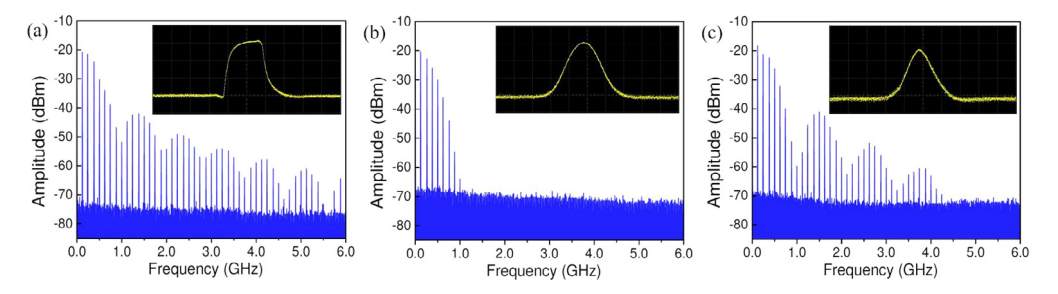


Fig. 8. Demonstration of the pulse shaping function based on the proposed RF spectral shaper. (a) RF spectrum of a square-like pulse that to be reshaped. (b) Reshaped into a Gaussian pulse through the low-pass equalization function. (c) Reshaped into a triangular pulse through the saw-tooth equalization function. Insets: Waveforms of the corresponding pulses in time domain, scale: 1 ns/div.

In this article, we experimentally demonstrated a highly reconfigurable microwave photonics-based RF spectral shaper for wideband gain/loss equalization and RF spectral shaping. The proposed scheme is based on the use of cascaded MZIs to achieve multiple tunable and reconfigurable RF spectral control points, where the spectral profile, amplitude, frequency, and spectral width can be adjusted. The demonstrated shaping functions include positive/negative linear slope compensation, parabolic and inverted parabolic equalizations, as well as complex and multiple-peak spectral shaping, with both compensation depth and slope being highly adjustable. The proposed RF spectral shaper can be used for dynamic frequency response equalization in RF system and arbitrary RF pulse shaping, which significant improvements in the functionality and operation flexibility are obtained when comparing with existing electronic counterparts. The wideband operation range and extraordinary reconfigurability of the proposed RF spectral shaper make it suitable for a variety of applications, including RF/microwave signal processing, spectrum shaping, and multiband communications.

# Acknowledgment

We would like to thank Prof. Paul Prucnal from Princeton University for providing the balanced photo-detector.

# **Funding**

National Science Foundation (NSF), USA (ECCS 1653525 and CMMI 1400100).

## References

- [1] J.P. Yao, Microwave photonics, J. Lightwave Technol. 27 (2009) 314-335.
- [2] Capmany, J. Mora, I. Gasulla, J. Sancho, J. Lloret, S. Sales, Microwave photonic signal processing, J. Lightwave Technol. 31 (2013) 571–586.
- [3] Q. Ma, M. Ma, Broadband amplifier gain slope equalization filter, Prog. Electromagnet. Res. Symp. 1AP (2008) 23–25.
- [4] H. Wang, B. Yan, Z. Wang, R.M. Xu, A broadband microwave gain equalizer, Prog. Electromagnet. Res. Lett. 33 (2012) 63–72.
- [5] L. Han, A reconfigurable microwave equalizer with different maximum attenuations based on RF MEMS switches, IEEE Sens. J. 16 (2016) 17–18.
- [6] G. Hueber, R.B. Staszewski, Multi-Mode/Multi-Band RF Transceivers for Wireless Communications: Advanced Techniques, Architectures, and Trends, John Wiley & Sons, 2011.
- [7] J. Mitola, Cognitive radio for flexible mobile multimedia communications, Mob. Multimedia Commun. MONET 6 (2001) 435–441.
- [8] E. Chai, K.G. Shin, J. Lee, S.J. Lee, R. Etkin, Fast spectrum shaping for next-generation wireless networks, IEEE Trans. Mob. Comput. 1 (2014) 1–1.
- [9] H.A. Mahmoud, H. Arslan, Spectrum shaping of OFDM-based cognitive radio signals, in: Radio and Wireless Symposium, 2008 IEEE, 2008, pp. 113–116.
- [10] A. Monmayrant, S. Weber, B. Chatel, A newcomer's guide to ultrashort pulse shaping and characterization, J. Phys. B 43 (2010) 103001.
- [11] P. Rulikowski, J. Barrett, Adaptive arbitrary pulse shaper, IEEE Microw. Compon. Lett. 18 (2008) 356–358.
- [12] C.F. Chen, T.Y. Huang, R.B. Wu, Design of dual-and triple-passband filters using alternately cascaded multiband resonators, IEEE Trans. Microw. Theory Techn. 54 (2006) 3550–3558.

- [13] K.W. Hsu, J.H. Lin, W.H. Tu, Compact sext-band bandpass filter with sharp rejection response, IEEE Microw. Compon. Lett. 24 (2014) 593–595.
- [14] Gómez-García, R. Guyette, A.C, Reconfigurable multi-band microwave filters, IEEE Trans. Microw. Theory Techn. 63 (2015) 1294–1307.
- [15] Y.S. Lin, C.C. Liu, K.M. Li, C.H. Chen, Design of an LTCC tri-band transceiver module for GPRS mobile applications, IEEE Trans. Microw. Theory Techn. 52 (2004) 2718–2724.
- [16] C.Y. Liou, S.G. Mao, Triple-band marchand balun filter using coupled-line admmittance inverter technique, IEEE Trans. Microw. Theory Techn. 61 (2013) 3846–3852
- [17] S.C. Lin, Microstrip dual/quad-band filters with coupled lines and quasi-lumped impedance inverters based on parallel-path transmission, IEEE Trans. Microw. Theory Techn. 59 (2011) 1937–1946.
- [18] J. Capmany, D. Novak, Microwave photonics combines two worlds, Nature Photon. 1 (2007) 319–330.
- [19] R.A. Minasian, Photonic signal processing of microwave signals, IEEE Trans. Microw. Theory Techn. 54 (2006) 832–846.
- [20] J.P. Yao, Photonics to the rescue: A fresh look at microwave photonic filters, IEEE Microw. Mag. 16 (2015) 46-60.
- [21] L.R. Chen, Silicon photonics for microwave photonic applications, in: Optical Fiber Communication Conference M2B.4, 2015.
- [22] J. Capmany, I. Gasulla, D. Pérez, Microwave photonics: the programmable processor, Nature Photon. 10 (2016) 6–8.
- [23] L. Zhuang, C.G.H. Roeloffzen, M. Hoekman, K. Boller, A.J. Lowery, Programmable photonic signal processor chip for radiofrequency applications, Optica 2 (2015) 854–859.
- [24] J.P. Yao, Microwave photonics: Arbitrary waveform generation, Nature Photon. 4 (2010) 79–80.
- [25] A.M. Weiner, Ultrafast optical pulse shaping: A tutorial review, Opt. Commun. 284 (2011) 3669–3692.
- [26] L.R. Chen, P. Moslemi, M. Ma, R. Adams, Simultaneous multi-channel microwave photonic signal processing, Photonics 4 (2017) 44.
- [27] M.H. Khan, H. Shen, Y. Xuan, L. Zhao, S. Xiao, D.E. Leaird, A.M. Weiner, M. Qi, Ultrabroad-bandwidth arbitrary radiofrequency waveform generation with a silicon photonic chip-based spectral shaper, Nature Photon. 4 (2010) 117–122.
- [28] F. Ferdous, H. Miao, D.E. Leaird, K. Srinivasan, J. Wang, L. Chen, L.T. Varghese, A.M. Weiner, Spectral line-by-line pulse shaping of on-chip microresonator frequency combs, Nature Photon. 5 (2011) 770–776.
- [29] C. Wang, J.P. Yao, Phase-coded millimeter-wave waveform generation using a spatially discrete chirped fiber bragg grating, IEEE Photon. Technol. Lett. 24 (2012) 1493–1495.
- [30] J. Li, Y. Dai, F. Yin, W. Li, M. Li, H. Chen, Xu. K., Megahertz-resolution programmable microwave shaper, Opt. Lett. 43 (2018) 1878–1881.
- [31] J. Sancho, J. Bourderionnet, J. Lloret, S. Combrié, I. Gasulla, S. Xavier, S. Sales, P. Colman, G. Lehoucq, D. Dolfi, J. Capmany, Integrable microwave filter based on a photonic crystal delay line, Nature Commun. 3 (2012) 1075.
- [32] V.R. Supradeepa, C.M. Long, R. Wu, F. Ferdous, E. Hamidi, D.E. Leaird, A.M. Weiner, Comb-based radiofrequency photonic filters with rapid tunability and high selectivity, Nature Photon. 6 (2012) 186–194.
- [33] D. Marpaung, B. Morrison, M. Pagani, R. Pant, D.Y. Choi, B. Luther-Davies, S.J. Madden, B.J. Eggleton, Low-power, chip-based stimulated brillouin scattering microwave photonic filter with ultrahigh selectivity, Optica 2 (2015) 76–83.
- [34] J. Mora, B. Ortega, A. Díez, J.L. Cruz, M.V. Andrés, J. Capmany, D. Pastor, Photonic microwave tunable single-bandpass filter based on a Mach–Zehnder interferometer, J. Lightwave Technol. 24 (2006) 2500.
- [35] J. Ge, H. Feng, G. Scott, M.P. Fok, High-speed tunable microwave photonic notch filter based on phase modulator incorporated Lyot filter, Opt. Lett. 40 (2015) 48–51.
- [36] E. Hamidi, D.E. Leaird, A.M. Weiner, Tunable programmable microwave photonic filters based on an optical frequency comb, IEEE Trans. Microw. Theory Techn. 58 (2010) 3269–3278.
- [37] X. Xue, Y. Xuan, H.J. Kim, J. Wang, D.E. Leaird, M. Qi, A.M. Weiner, Programmable single-bandpass photonic RF filter based on Kerr comb from a microring, J. Lightwave Technol. 32 (2014) 3557–3565.

- [38] J. Mora, L.R. Chen, J. Capmany, Single-bandpass microwave photonic filter with tuning and reconfiguration capabilities, J. Lightwave Technol. 26 (2008) 2663–2670.
- [39] J. Ge, M.P. Fok, Optically controlled fast reconfigurable microwave photonic dual-band filter based on nonlinear polarization rotation, IEEE Trans. Microw. Theory Techn. 65 (2017) 253–259.
- [40] W. Wei, L. Yi, Y. Jaouën, W. Hu, Software-defined microwave photonic filter with high reconfigurable resolution, Sci. Rep. 6 (2016) 35621.
- [41] J. Ge, M.P. Fok, Passband switchable microwave photonic multiband filter, Sci. Rep. 5 (2015) 15882.
- [42] X. Zhu, F. Chen, H. Peng, Z. Chen, Novel programmable microwave photonic filter with arbitrary filtering shape and linear phase, Opt. Express 25 (2017) 9232–9243
- [43] M.P. Fok, J. Ge, Tunable multiband microwave photonic filters, Photonics 4 (2017) 45.
- [44] L. Gao, J. Zhang, X. Chen, J.P. Yao, Microwave photonic filter with two independently tunable passbands using a phase modulator and an equivalent phase-shifted fiber Bragg grating, IEEE Trans. Microw. Theory Techn. 62 (2014) 280, 287
- [45] H. Chen, Z. Xu, H. Fu, S. Zhang, C. Wu, H. Wu, H. Xu, Z. Cai, Switchable and tunable microwave frequency multiplication based on a dual-passband microwave photonic filter, Opt. Express 23 (2015) 9835–9843.
- [46] H.J. Kim, D.E. Leaird, A.M. Weiner, Rapidly tunable dual-comb RF photonic filter for ultrabroadband RF spread spectrum applications, IEEE Trans. Microw. Theory Techn. 64 (2016) 3351–3362.

- [47] Y. Jiang, P.P. Shum, P. Zu, J. Zhou, G. Bai, J. Xu, Z. Zhou, H. Li, S. Wang, A selectable multiband bandpass microwave photonic filter, IEEE Photon. J. 5 (2013) 5500509–5500509.
- [48] Q. Liu, J. Ge, M.P. Fok, Microwave photonic multiband filter with independently tunable passband spectral properties, Opt. Lett. 43 (2018) 5685–5688.
- [49] J. Ge, M.P. Fok, Reconfigurable RF multiband filter with widely tunable passbands based on cascaded optical interferometric filters, J. Lightwave Technol. 36 (2018) 2933–2940.
- [50] X. Xue, X. Zheng, H. Zhang, B. Zhou, Highly reconfigurable microwave photonic single-bandpass filter with complex continuous-time impulse responses, Opt. Express 20 (2012) 26929–26934.
- [51] J. Ge, M.P. Fok, Continuously tunable and reconfigurable microwave photonic multiband filter based on cascaded MZIs, in: IEEE Photonics Conference, WA1, Orlando, FL, 2017.
- [52] D. Pérez, I. Gasulla, L. Crudgington, D.J. Thomson, A.Z. Khokhar, K. Li, W. Cao, G.Z. Mashanovich, J. Capmany, Multipurpose silicon photonics signal processor core, Nature Comm. 8 (2017) 636.
- [53] B. Guan, S.S. Djordjevic, N.K. Fontaine, L. Zhou, S. Ibrahim, R.P. Scott, D.J. Geisler, Z. Ding, S.B. Yoo, CMOS compatible reconfigurable silicon photonic lattice filters using cascaded unit cells for RF-photonic processing, IEEE J. Sel. Top. Quantum Electron. 20 (2014) 359–368.
- [54] J.S. Fandino, P. Munoz, D. Domenech, J. Capmany, A monolithic integrated photonic microwave filter, Nature Photon. 11 (2017) 124–129.
- [55] D. Pérez, I. Gasulla, J. Capmany, Software-defined reconfigurable microwave photonics processor, Opt. Express 23 (2015) 14640–14654.
- [56] W. Liu, M. Li, R.S. Guzzon, E.J. Norberg, J.S. Parker, M. Lu, L.A. Coldren, Yao. J., A fully reconfigurable photonic integrated signal processor, Nature Photon. 10 (2016) 190.